HHS Public Access

Author manuscript

Mol Cancer Ther. Author manuscript; available in PMC 2019 January 07.

Published in final edited form as:

Mol Cancer Ther. 2018 June ; 17(6): 1207–1216. doi:10.1158/1535-7163.MCT-17-1267.

The DNA-PK Inhibitor VX-984 Enhances the Radiosensitivity of Glioblastoma Cells Grown *In Vitro* and as Orthotopic Xenografts

Cindy R. Timme, **Barbara H. Rath**, **John W. O'Neill**, **Kevin Camphausen**, and **Philip J. Tofilon**

Radiation Oncology Branch, National Cancer Institute, Bethesda, Maryland.

Abstract

Radiotherapy is a primary treatment modality for glioblastomas (GBM). Because DNA-PKcs is a critical factor in the repair of radiation-induced double strand breaks (DSB), this study evaluated the potential of VX-984, a new DNA-PKcs inhibitor, to enhance the radiosensitivity of GBM cells. Treatment of the established GBM cell line U251 and the GBM stem-like cell (GSC) line NSC11 with VX-984 under *in vitro* conditions resulted in a concentration-dependent inhibition of radiation-induced DNAPKcs phosphorylation. In a similar concentration-dependent manner, VX-984 treatment enhanced the radiosensitivity of each GBM cell line as defined by clonogenic analysis. As determined by γH2AX expression and neutral comet analyses, VX-984 inhibited the repair of radiation-induced DNA double-strand break in U251 and NSC11 GBM cells, suggesting that the VX-984-induced radio-sensitization is mediated by an inhibition of DNA repair. Extending these results to an *in vivo* model, treatment of mice with VX-984 inhibited radiation-induced DNA-PKcs phosphorylation in orthotopic brain tumor xenografts, indicating that this compound crosses the blood–brain tumor barrier at sufficient concentrations. For mice bearing U251 or NSC11 brain tumors, VX-984 treatment alone had no significant effect on overall survival; radiation alone increased survival. The survival of mice receiving the combination protocol was significantly increased as compared with control and as compared with radiation alone. These results indicate that VX-984 enhances the radiosensitivity of brain tumor xenografts and suggest that it may be of benefit in the therapeutic management of GBM.

Introduction

A primary treatment modality for glioblastoma (GBM) is radiotherapy, which is typically used in combination with surgery and temozolomide. Despite this combined treatment, median survival rates for GBM remain at 12 to 15 months after diagnosis (1). Although they can be extensively invasive, GBMs usually recur in the initial radiation treatment volume (1–

Corresponding Author: Philip J. Tofilon, National Cancer Institute, 10 Center Drive-MSC1002, Building 10, B3B69B, Bethesda, MD 20892. Phone: 240-858-3048; Fax: 240-541-4525; tofilonp@mail.nih.gov.

Authors' Contributions

Conception and design: C.R. Timme, K. Camphausen, P.J. Tofilon Development of methodology: C.R. Timme, P.J. Tofilon Acquisition of data (provided animals, acquired and managed patients, provided facilities, etc.): C.R. Timme, B.H. Rath, J.W. O'Neill Analysis and interpretation of data (e.g., statistical analysis, biostatistics, computational analysis): C.R. Timme, B.H. Rath, K. Camphausen, P.J. Tofilon Writing, review, and/or revision of the manuscript: C.R. Timme, K. Camphausen, P.J. Tofilon Administrative, technical, or material support (i.e., reporting or organizing data, constructing databases): P.J. Tofilon Study supervision: P.J. Tofilon

Disclosure of Potential Conflicts of Interest

No potential conflicts of interest were disclosed.

3). This local failure pattern is indicative of radioresistance and suggests that the therapeutic response of GBM could be improved by the addition of a radiosensitizer. A source of potential targets for GBM radio-sensitization are molecules participating in the repair of DNA double-strand breaks (DSB), the lesion primarily responsible for radiation-induced cell death.

In solid tumor cells, a critical process mediating DSB repair is nonhomologous end-joining (NHEJ), which results in the direct ligation of broken DNA strands and operates throughout the cell cycle (except during mitosis; ref. 4). An essential component of NHEJ is DNA-dependent protein kinase (DNA-PK), which is composed of a catalytic serine/threonine protein kinase (DNA-PKcs/PRKDC) and a Ku heterodimer (Ku70 and Ku80; refs. 4, 5). NHEJ is initiated by binding of the Ku heterodimer to the exposed ends of a DSB followed by recruitment of DNA-PKcs, which results in activation of its kinase activity and subsequent autophosphorylation. This process leads to the recruitment of the other NHEJ components and ultimately DSB ligation (4). Cells deficient in Ku or DNAPKcs have significantly diminished DSB repair capacity and are radiosensitive (5). DNA-PKcs was initially linked to GBM radiosensitivity by studies on the M059J and M059K cell lines, which were isolated from different areas of a human GBM biopsy specimen (6). The DNA-PKcs–deficient M059J cells are highly radiosensitive compared with the DNA-PK-proficient M059K cell line. Introduction of a fragment of human chromosome 8 that contains the DNA-PKcs gene reduced the radiosensitivity of M059J (7); treatment with the DNA-PKcs inhibitor NU7026 increased the radiosensitivity of M059K but not M059J cells (8, 9). Combined with its established role in NHEJ, these data implicate DNA-PKcs as a potential target for GBM radiosensitization.

A number of small molecule inhibitors of DNA-PKcs have been developed and shown to be effective radiosensitizers *in vitro* (10). However, in general, they suffer from poor *in vivo* pharmacokinetics and bioavailability, which limits their clinical applicability (10). Moreover, as compared with other tumor sites, drugs targeting GBM must confront the additional pharmacokinetic obstacle of the blood–brain tumor barrier (BBTB; refs. 11, 12). Toward identifying an inhibitor appropriate for GBM therapy, we have investigated the radiosensitizing potential of VX-984 (13), a new ATP-competitive DNA-PKcs inhibitor. The data presented here show that the VX-984 inhibits radiation-induced DNA-PKcs phosphorylation and DSB repair in GBM cells grown under *in vitro* conditions, effects that are accompanied by an increase in radiosensitivity. VX-984 is also shown to inhibit radiation-induced DNA-PKcs phosphorylation in orthotopic brain tumor xenografts. Although VX-984 treatment had no effect on the survival of mice bearing orthotopic brain tumors, it did enhance the radiation-induced prolongation of survival. These results suggest that the combination of VX-984 and radiotherapy may improve GBM therapeutic response.

Materials and Methods

Cell lines and treatments

The U251 human GBM cell line was obtained from the Division of Cancer Treatment and Diagnosis Tumor Repository (DCTD), National Cancer Institute (NCI) grown in Dulbecco’s Modified Eagle Medium (DMEM) supplemented with 10% fetal bovine serum (FBS,

Invitrogen), and maintained in an atmosphere of 5% CO_2/95% air at 37° C. U251 cells were cultured less than 3 months after resuscitation and were last authenticated in May 2015 by STR analysis (Indexx Laboratories). The glioblastoma stem-like cell (GSC) line NSC11 (kindly provided by Dr. Frederick Lang, MD Anderson Cancer Center) was isolated from human GBM surgical specimens as previously described (14). Neurospheres were maintained in stem cell medium consisting of DMEM/F-12 (Invitrogen), B27 supplement (Invitrogen), and human recombinant bFGF and EGF (50 ng/mL each, R&D Systems) at 37 C, 5%CO_2/5%O_2. $CD133^+$ NSC11 cells were isolated from neurosphere cultures by fluorescence-activated cell sorting (FACS) as reported previously (15). All $CD133^+$ NSC11 cells met the criteria for tumor stem-like cells including self-renewal, differentiation along glial and neuronal pathways, expression of stem cell related genes, and formation of brain tumors when implanted in immunodeficient mice (15). For use in an *in vitro* experiment, $CD133^+$ NSC11 neurosphere cultures were disaggregated into single cells as described (15) and seeded onto poly-L-ornithine (Invitrogen)/laminin (Sigma-Aldrich) coated tissue culture dishes in stem cell media. Under these conditions, single-cell GSCs attach and grow as an adherent monolayer maintaining their $CD133^+$ expression and stem-line characteristics (16). NSC11 cells were cultured less than 2 months after resuscitation. Both U251 and NSC11 cells tested negative for mycoplasma contamination by PCR analysis (Indexx Laboratories). Radiation was delivered using a 320 kV X-ray machine (Precision X-Ray Inc.) with a 2.0 mm aluminum filtration (300 kV peak; 10 mA) at a dose rate of 2.3 Gy/minute; control cultures were mock irradiated. All *in vitro* experiments were performed using the same machine (*in vivo* experiments use a separate X-ray machine); output and quality assurance are performed annually. VX-984 was obtained from Vertex Pharmaceuticals Inc. and reconstituted in dimethyl sulfoxide (DMSO) for *in vitro* experiments.

Immunoblot analysis

For *in vitro* experiments, protein was collected and subjected to immunoblot analyses as previously described (17). For *in vivo* experiments, GFP-positive human tumor tissue was dissected from the mouse brain and snap frozen in liquid nitrogen. Samples were homogenized (Polytron Brinkman) in lysis buffer (17) and incubated for 0.5 hour at 4°C; protein was subjected to immunoblot analyses as previous described (17). Anti-phospho-DNAPK (Ser2056; #ab14918) was obtained from Abcam. Anti-total-DNA-PK was obtained from Thermo-Fisher Scientific. Anti-b-actin and anti-Sox2 (human-specific, #D6D9) were obtained from Cell Signaling Technology. Donkey anti-rabbit and sheep anti-mouse horseradish peroxidase-conjugated secondary antibodies were purchased from GE Healthcare Life Sciences. Bands were quantified by densitometry analysis using Image Studio Lite (LICOR Biosciences).

Clonogenic survival assay

U251 cells growing in monolayer were disaggregated into a single-cell suspension and seeded onto tissue culture plates. NSC11 $CD133^+$ neurospheres were disaggregated into single cells and seeded onto tissue culture plates coated with poly-L-lysine (Invitrogen) as previously described, which allows for adherent colony formation (15). To evaluate radiosensitivity, cells were plated at clonal density in 6-well plates and irradiated the next day. Ten to 18 days after irradiation, plates were stained with 0.5% crystal violet, the number

of colonies determined, and the surviving fractions were calculated. Radiation survival curves were generated after normalizing for the cytotoxicity induced by VX-984. The data presented are the mean ± SEM of 3 independent experiments.

Immunofluorescent analysis of γH2AX foci

To visualize foci, cells grown in chamber slides were fixed with 10% neutral buffered formalin (NBF), permeabilized with 0.1% Triton X-100, and blocked with 1% bovine serum albumin in PBS containing 5% FBS. The slides were incubated with antibody to phospho-H2AX (Millipore) followed by incubation with anti-mouse-AlexaFluor488 (Invitrogen) and mounted with Prolong Diamond antifade reagent containing DAPI (Invitrogen) to visualize nuclei. Images were captured on a Zeiss upright fluorescent microscope equipped with a 63 ×oil immersion lens. Automated image analysis to determine the number of foci per nucleus was performed using ZEN software with the advanced Image Processing and Analysis module (Zeiss). Foci determination was quantified in at least 30 cells per condition. Data presented are the mean ± SEM of 3 independent experiments.

Neutral comet assay

The neutral comet assay was performed using a commercially available kit according to the recommendations from the manufacturer (Trevigen) with slight modifications. Briefly, mono-layers were irradiated (10 Gy) and returned to the incubator. At specified times, single-cell suspensions were generated, washed with PBS, mixed with low melting agarose (1:10), and transferred to the provided slides. Cells were lysed at 4°C for 1 hour on wet ice, subjected to electrophoresis for 20 minutes at room temperature and fixed with 70% EtOH. DNA was stained with SYBR Green, and digital fluorescent images were analyzed with TriTek CometScore as described (18). Data are expressed as % damage remaining in which the Olive tail moment from cultures irradiated on ice and collected immediately after irradiation was set to 100% damage, with the remaining times after irradiation normalized accordingly. All time points were corrected for VX-984 or vehicle treatment alone by subtracting the Olive tail moment of sham irradiated vehicle or VX-984–treated samples. At least 50 cells per condition were measured. Data presented are the mean ± SEM of 3 independent experiments.

Orthotopic xenografts

U251 (2.5×10^5) cells or $CD133^+$ NSC11 cells (1.0×10^5) transduced to express luciferase and GFP with the lentivirus LVpFUGQ-UbC-ffLuc2-eGFP2 (19) were intracranially implanted into the right striatum of 6- to 8-week-old athymic female nude mice (Ncr nu/nu; NCI Animal Production Program) at 1.0 mm anterior and 2.0 mm lateral to the bregma to a depth of 3.0 mm as previously described (19). Bioluminescent imaging (BLI) and local irradiation were all performed as described previously (19). VX-984 was dissolved in freshly made 5% methylcellulose and delivered by oral gavage. On day 6 (U251) or day 20 (NSC11) after implantation, consistent BLI was detected in all mice, which were then randomized according to the signal obtained from BLI into four groups: vehicle, VX-984, radiation (3 × 3 Gy), and VX-984 plus radiation (7–8 mice/group), and the treatments initiated the next day. Three Gy was delivered on 3 consecutive days with VX-984 (dissolved in 5% methylcellulose) delivered by oral gavage each day 0.5 hour before and 4

hours after irradiation. For irradiation, mice were anesthetized using a cocktail of keta-mine/xylazine/acepromazine and placed in well-ventilated Plexi glass jigs with shielding for the entire torso of the mouse along with critical normal structures of the head (ears, eyes, and neck). Radiation was delivered using an X-Rad 320 X-irradiator (Precision X-Rays, Inc.) with a 2.0 mm aluminum filtration (300 kV peak; 10 mA) X-ray at a dose rate of 2.9 Gy/minute. All *in vivo* irradiation experiments were performed using the same instrument located within the animal facility; output and quality assurance are performed annually. Mice were monitored every day until the onset of neurologic symptoms (morbidity). BLI and weights were measured biweekly (U251) or weekly (NSC11) after irradiation until the first mouse of the group was lost. All experiments were performed as approved by the principles and procedures in the NIH Guide for Care and Use of Animals and conducted in accordance with the Institutional Animal Care and Use Committee.

Statistical analysis

For *in vitro* experiments, statistical significance was determined using a two-tailed Student *t* test. For *in vivo* studies, statistical significance was determined using a one-tailed Student *t* test for immunoblot analyses. For *in vivo* survival studies, Kaplan–Meier survival curves were generated and log-rank values calculated. Statistical significance of median survivals was calculated using Mann–Whitney test. Values of $P < 0.05$ were considered significant.

Results

DNA-PKcs phosphorylation at Ser2056 is typically used as an indicator of its activation in human cells (20). Thus, initial studies defined the effects of VX-984 on radiation-induced DNA-PKcs phosphorylation in two representative models of GBM: U251 cells, a long established GBM cell line, and NSC11, a primary GBM stem-like cell line (GSC). For these experiments, VX-984 was added to culture media at the indicated concentration 1 hour before irradiation with cells collected for immunoblot analysis 1 hour after irradiation. Because NSC11 cells are more radiosensitive than U251 cells as measured by clonogenic analysis (15), to evaluate DNA-PKcs phosphorylation at similar survival levels, NSC11 and U251 cells were irradiated with 6 and 10 Gy, respectfully. As shown in Fig. 1A and B, whereas DNA-PKcs phosphor-ylation was induced after irradiation of U251 and NSC11 cells, consistent with previous reports using other cell lines (20), VX-984 treatment alone had no effect. When VX-984 was delivered 1 hour before irradiation, there was a concentration-dependent decrease in radiation-induced DNA-PKcs phosphorylation in each glioma line. Neither treatment nor the combination altered levels of total DNA-PKcs.

The effect of VX-984 on the radiosensitivity of U251 and NSC11 was determined using a clonogenic survival assay. For this analysis, VX-984 was added to culture media 1 hour before irradiation; 24 hours after irradiation the media were replaced with fresh, drug-free media and colonies determined after 10 to 12 days (U251) or 16 to 18 days (NSC11). As shown in Fig. 2A, VX-984 enhanced the radiosensitivity of U251 cells in a concentration-dependent manner with DEFs (dose enhancement factor at a surviving fraction of 0.10) of 1.4 and 2.1 at 100 and 250 nmol/L, respectively. Surviving fractions after VX-984 exposure alone were 1.14 ± 0.03 and 1.07 ± 0.09 at 100 and 250 nmol/L, respectively. The

radiosensitivity of NSC11 cells was also increased in a concentration-dependent manner by VX-984 (Fig. 2B), with DEFs of 1.1, 1.5, and 1.9 at 100, 250, and 500 nmol/L, respectively. Surviving fractions after VX-984 exposure alone were 1.05 0.08, 0.94 ± 0.09 and 0.95 ± 0.09 at 100, 250, and 500 nmol/L, respectively. These results indicate that although VX-984 alone has no effect of clonogenic survival, it enhances the radiosensitivity of GBM cells.

Because VX-984 was added 1 hour before irradiation, redistribution into a radiosensitive phase of the cell cycle is unlikely to account for the observed radiosensitization. Therefore, toward to defining the mechanism responsible, we focused on the putative role of DNA-PKcs in the repair of radiation-induced DSBs. To determine whether this is the mechanism through which VX-984 enhances the radiosensitivity of GBM cells, DSB repair was evaluated in U251 and NSC11 cells using γH2AX foci and neutral comet analyses. The level of radiation-induced DSBs corresponds to the number of γH2AX foci induced per cell whereas γH2AX dispersal correlates with DSB repair (21). To assess the effect of VX-984 on DSB induction and repair, γH2AX foci were determined as a function time after irradiation (2 Gy). Specifically, VX-984 was added to culture media 1 hour prior to irradiation with cells collected for foci determination at the specified times after irradiation. Initial experiments established that after irradiation, γH2AX foci levels in U251 and NSC11 cells return to unirradiated levels by 16 and 24 hours, respectively, which were then used as the latest time points evaluated. For both U251 and NSC11, VX-984 had no effect on the number of radiation-induced γH2AX foci at 1 hour, suggesting that VX-984 had no effect on the initial level of radiation-induced DSBs (Fig. 3A and B). However, at 16 hours for U251 and 24 hours for NSC11 following irradiation, a significant increase in the number of γHA2X foci was detected in VX-984–treated cells compared with vehicle alone. The persistence of γH2AX foci in irradiated cells that were treated with VX-984 suggests an inhibition of DNA DSB repair. For the neutral comet assay VX-984 was added to culture media 1 hour before exposure to 10 Gy and cells collected for analysis at times out to 24 hours after irradiation (Fig. 3C and D). For both cell lines, VX-984 treatment significantly slowed the repair of radiation-induced DSBs, which was detectable by 3 hours. The DSBs remaining at 24 hours reflect residual radiation-induced damage, which was increased in VX-984–treated cells, and is consistent with an increase in radiation-induced cell death. Thus, data generated from the γH2AX and neutral comet assays indicate that VX-984 inhibits the repair of radiation-induced DSBs and suggests that this is the mechanism mediating the observed radiosensitization.

To determine whether the VX-984–mediated radiosensitization extends to a relevant *in vivo* model, we used orthotopic brain tumor xenografts. First, the ability of VX-984 to inhibit radiation-induced DNA-PKcs phosphorylation was tested in U251 intracerebral xenografts. VX-984 (100 mg/kg) was delivered by oral gavage at 1 or 4 hours before irradiation; 1 hour after irradiation tumors were harvested and subjected to immunoblot analysis (Fig. 4A and B). In these studies, Sox2 expression, which is specific for the human tumor cells, was used as a loading control. As shown, 10 Gy resulted in a significant induction of DNA-PKcs phosphorylation in the U251 tumors. VX-984 treatment 4 hours before irradiation prevented the increase in DNA-PKcs phosphor-ylation with a similar degree of inhibition achieved when the drug was delivered only 1 hours prior to 10 Gy. In an independent experiment (Fig.

4C and D), we compared the effects of 50 and 100 mg/kg VX-984 delivered 4 hours before irradiation on DNAPKcs phosphorylation. Both doses of VX-984 reduced the levels DNA-PKcs phosphorylation after irradiation. These results indicate that VX-984 penetrates the BBTB to inhibit radiation-induced DNA-PKcs phosphorylation in brain tumor xenografts and that this inhibitory activity continues out to at least 4 hours after drug treatment.

Based on these results, a protocol was designed to test the antitumor effectiveness of the VX-984/radiation combination. For U251 tumors, at 6 days after intracerebral implant mice were randomized according to BLI signal into 4 groups: vehicle (control), radiation (3 Gy), VX-984 (50 mg/kg), and VX-984 plus radiation and treatment begun the following day. VX-984 was delivered twice a day (50 mg/kg, oral gavage) at 30 minutes before and 4 hours following local irradiation of the tumor (3 Gy) for 3 consecutive days (3 × 3 Gy). Mice were followed until the initial onset of morbidity and survival curves generated. In addition, BLI was performed on each treatment group until the initial mouse in that group was designated as morbid. VX-984 alone had no effect on U251 growth rate, reflected by BLI ratio, as compared with control; radiation alone resulted in a growth delay, which was increased in the combination treatment (Fig. 5A). As shown in Fig. 5B, VX-984 treatment of U251 tumors alone had no significant effect on overall survival as compared with vehicle; radiation alone resulted in an increase in survival. The survival of mice receiving the combination protocol was significantly increased as compared with vehicle and, importantly, as compared with radiation alone. The median survival times for the treatment groups are shown in the boxplots in Fig. 5C. Whereas the median survival after VX-984 was the same as vehicle, radiation alone increased median survival by 14 days and the combination by 32 days versus vehicle, indicating that the combination protocol increased tumor radiosensitivity with an apparent DEF of 2.3. VX-984 alone did not adversely affect mouse weight nor did the combination protocol as compared with vehicle (Fig. 5D).

The same protocol was applied to NSC11 brain tumors with randomization according to BLI on day 20 after implant. VX-984 alone had no effect on NSC11 growth rate, reflected by BLI ratio, as compared with control; radiation alone resulted in a minimal growth delay, which was increased in the combination treatment (Fig. 6A). As shown in Fig. 6B, VX-984 treatment of NSC11 tumors alone had no effect on overall survival as compared with vehicle; radiation alone resulted in a nonsignificant increase in survival. The survival of mice receiving the combination protocol, however, was significantly increased as compared with vehicle and, importantly, as compared with radiation alone. The median survival times for the treatment groups are shown in the boxplots in Fig. 6C. Whereas the median survival after VX-984 was increased by 1 day as compared with vehicle, radiation alone increased median survival by 10 days and the combination by 21 days versus vehicle, indicating that the combination protocol increased tumor radiosensitivity with an apparent DEF of 2.0. VX-984 alone did not adversely affect mouse weight nor did the combination protocol as compared with vehicle (Fig. 6D). Thus, these results indicate that VX-984 enhances the radiosensitivity of 2 GBM orthotopic xenograft models.

Discussion

Glioblastoma recurrence following radiotherapy occurs at an extremely high rate and within the initial radiation treatment volume, indicating that GBM cells *in situ* are highly radioresistant (22). One approach to developing agents that may overcome GBM radioresistance is to target molecules involved in the repair of radiation-induced DSBs, which in solid human tumors primarily occurs through the NHEJ pathway (23, 24). Initiation of NHEJ is dependent on DNA-PK, which is composed of DNA-binding proteins and the more readily targetable kinase DNAPKcs. In support of DNA-PKcs as a potential target for radio-sensitization, its knockdown using siRNA was shown to enhance the radiosensitivity of liver, bone, colon, and oral cancer cell lines (25–27). The significance of its kinase domain in radiosensitivity was established using a panel of Chinese hamster ovarian (CHO) cell lines that contained site-directed mutation(s) that abolished the kinase activity of DNA-PKcs; each of these cell lines was extremely radiosensitive as compared with parental controls (28). Consistent with laboratory results, clinical studies also suggested a role for DNA-PKcs as a determinant of therapeutic response. Increased expression or activity of DNA-PKcs has been reported to correlate with poor overall survival of patients with B-cell chronic lymphocytic leukemia, ovarian, liver cancer, and neuroblastoma (29–32). With respect to the response to radio-therapy, elevated DNA-PKcs expression was reported to correlate with recurrence of prostate tumors (33, 34) and decreased survival of patients with GBM (35). These studies thus implicate DNAPKcs as a potential target for tumor radiosensitization.

Toward translating this information into the clinic, small molecule inhibitors selective for DNA-PKcs have been developed (10). Whereas such inhibitors have been shown to enhance the *in vitro* radiosensitivity of a variety of human tumor cell lines including glioma (32, 36–40), whether any cross the blood–brain tumor barrier at sufficient concentrations and are thus suitable for GBM treatment has not been reported. As shown here, VX-984 inhibits the radiation-induced DNAPKcs phosphorylation in human GBM cell lines *in vitro*, which is accompanied by an inhibition of DSB repair and enhanced radiosensitivity. These results are similar to those reported for other DNA-PKcs inhibitors on the *in vitro* radioresponse of human tumor cell lines. However, in addition to *in vitro* analyses, we extended the VX-984 experiments to an *in vivo* brain tumor model. Initially, the oral administration of VX-984 to mice was shown to inhibit the radiation-induced DNA-PKcs phosphorylation in orthotopic brain tumor xenografts, indicative of the drug penetrating the blood–brain tumor barrier at the necessary concentration. Targeting of DNA-PKcs with VX-984 under these orthotopic conditions was then shown to enhance the radiation-induced brain tumor growth delay and the radiation-induced prolongation of survival.

Because DNA-PKcs has been defined as a critical component of NHEJ, a potential complication of the VX-984/radiation combination is enhanced normal tissue toxicity. Along these lines, Dong and colleagues reported that the DNA-PKcs inhibitor NU7441 enhanced the *in vitro* radiosensitivity of mouse embryonic fibro-blasts as measured by a clonogenic assay (41). In contrast, using proliferation as a measure of radiosensitivity, the DNA-PKcs inhibitor NU7026 was reported to enhance the radiosensitivity of human neuroblastoma cell lines, but not normal human fibroblast cell lines (32). Given that the brain is composed

primarily of noncycling cells, the relevance of these *in vitro* results to the potential normal tissue toxicity after brain irradiation is unclear. However, in the studies presented here, there was no excessive weight loss detected in mice receiving VX-984/radiation combination protocol. Moreover, no acute skin toxicity on the head (site of irradiation) was observed during or after the treatment. Although no overt toxicity attributed to VX-984 was detected in these experiments using immunodeficient athymic nude mice, given that VX-984 penetrates the blood–brain tumor barrier, additional studies, including the use of immunocompe-tent mice, may be required to determine whether VX-984 enhances radiation-induced CNS injury.

In this study, we showed that VX-984 significantly enhanced the antitumor effectiveness of a fractionated irradiation protocol in two orthotopic GBM models. VX-984 administration alone did not affect tumor growth rate or the survival of tumor bearing mice, indicating that this DNA-PKcs inhibitor operates as a classic radiosensitizing agent (42). VX-984 is currently undergoing a First-in-Human Clinical Trial as a single agent and in combination with pegylated liposomal doxorubicin against advanced solid tumors. The results presented here suggest that delivery of this DNA-PKcs inhibitor in combination with radiotherapy may improve GBM treatment response.

Acknowledgments

The authors thank Division of Basic Sciences, Intramural Program, National Cancer Institute (Z1ABC011372) for support.

The costs of publication of this article were defrayed in part by the payment of page charges. This article must therefore be hereby marked *advertisement* in accordance with 18 U.S.C. Section 1734 solely to indicate this fact.

References

1. Stupp R, Mason WP, van den Bent MJ, Weller M, Fisher B, Taphoorn MJ, et al. Radiotherapy plus concomitant and adjuvant temozolomide for glioblastoma. N Engl J Med 2005;352:987–96. [PubMed: 15758009]
2. De Bonis P, Anile C, Pompucci A, Fiorentino A, Balducci M, Chiesa S, et al. The influence of surgery on recurrence pattern of glioblastoma. Clin Neurol Neurosurg 2013;115:37–43. [PubMed: 22537870]
3. Rapp M, Baernreuther J, Turowski B, Steiger HJ, Sabel M, Kamp MA. Recurrence pattern analysis of primary glioblastoma. World Neurosurg 2017;103:733–40. [PubMed: 28434963]
4. Davis AJ, Chen BP, Chen DJ. DNA-PK: a dynamic enzyme in a versatile DSB repair pathway. DNA Repair (Amst) 2014;17:21–9. [PubMed: 24680878]
5. Smith GC, Jackson SP. The DNA-dependent protein kinase. Genes Dev 1999;13:916–34. [PubMed: 10215620]
6. Lees-Miller SP, Godbout R, Chan DW, Weinfeld M, Day RS, 3rd, Barron GM, et al. Absence of p350 subunit of DNA-activated protein kinase from a radiosensitive human cell line. Science 1995;267: 1183–5. [PubMed: 7855602]
7. Hoppe BS, Jensen RB, Kirchgessner CU. Complementation of the radio-sensitive M059J cell line. Radiat Res 2000;153:125–30. [PubMed: 10629611]
8. Tavecchio M, Munck JM, Cano C, Newell DR, Curtin NJ. Further characterisation of the cellular activity of the DNA-PK inhibitor, NU7441, reveals potential cross-talk with homologous recombination. Cancer Chemother Pharmacol 2012;69:155–64. [PubMed: 21630086]

9. Liu Y, Zhang L, Liu Y, Sun C, Zhang H, Miao G, et al. DNA-PKcs deficiency inhibits glioblastoma cell-derived angiogenesis after ionizing radiation. J Cell Physiol 2015;230:1094–103. [PubMed: 25294801]
10. Pospisilova M, Seifrtova M, Rezacova M. Small molecule inhibitors of DNA-PK for tumor sensitization to anticancer therapy. J Physiol Pharmacol 2017;68:337–44. [PubMed: 28820390]
11. Zhou W, Chen C, Shi Y, Wu Q, Gimple RC, Fang X, et al. Targeting glioma stem cell-derived pericytes disrupts the blood–tumor barrier and improves chemotherapeutic efficacy. Cell Stem Cell 2017;21: 591–603e4. [PubMed: 29100012]
12. van Tellingen O, Yetkin-Arik B, de Gooijer MC, Wesseling P, Wurdinger T, de Vries HE. Overcoming the blood–brain tumor barrier for effective glioblastoma treatment. Drug Resist Updat 2015;19:1–12. [PubMed: 25791797]
13. Harnor SJ, Brennan A, Cano C. Targeting DNA-dependent protein kinase for cancer therapy. ChemMedChem 2017;12:895–900. [PubMed: 28423228]
14. Singh SK, Hawkins C, Clarke ID, Squire JA, Bayani J, Hide T, et al. Identification of human brain tumour initiating cells. Nature 2004;432: 396–401. [PubMed: 15549107]
15. McCord AM, Jamal M, Williams ES, Camphausen K, Tofilon PJ. CD133^{+} glioblastoma stem-like cells are radiosensitive with a defective DNA damage response compared with established cell lines. Clin Cancer Res 2009;15:5145–53. [PubMed: 19671863]
16. Pollard SM, Yoshikawa K, Clarke ID, Danovi D, Stricker S, Russell R, et al. Glioma stem cell lines expanded in adherent culture have tumor-specific phenotypes and are suitable for chemical and genetic screens. Cell Stem Cell 2009;4:568–80. [PubMed: 19497285]
17. Rath BH, Fair JM, Jamal M, Camphausen K, Tofilon PJ. Astrocytes enhance the invasion potential of glioblastoma stem-like cells. PLoS One 2013;8: e54752. [PubMed: 23349962]
18. Collins AR. The comet assay for DNA damage and repair: principles, applications, and limitations. Mol Biotechnol 2004;26:249–61. [PubMed: 15004294]
19. Jamal M, Rath BH, Tsang PS, Camphausen K, Tofilon PJ. The brain microenvironment preferentially enhances the radioresistance of CD133(+) glioblastoma stem-like cells. Neoplasia 2012;14: 150–8. [PubMed: 22431923]
20. Chen BP, Chan DW, Kobayashi J, Burma S, Asaithamby A, Morotomi-Yano K, et al. Cell cycle dependence of DNA-dependent protein kinase phosphorylation in response to DNA double strand breaks. J Biol Chem 2005;280:14709–15. [PubMed: 15677476]
21. Mah LJ, El-Osta A, Karagiannis TC. gammaH2AX: a sensitive molecular marker of DNA damage and repair. Leukemia 2010; 24:679–86. [PubMed: 20130602]
22. Milano MT, Okunieff P, Donatello RS, Mohile NA, Sul J, Walter KA, et al. Patterns and timing of recurrence after temozolomide-based chemoradiation for glioblastoma. Int J Radiat Oncol Biol Phys 2010; 78:1147–55. [PubMed: 20207495]
23. Takata M, Sasaki MS, Sonoda E, Morrison C, Hashimoto M, Utsumi H, et al. Homologous recombination and non-homologous end-joining pathways of DNA double-strand break repair have overlapping roles in the maintenance of chromosomal integrity in vertebrate cells. EMBO J 1998; 17:5497–508. [PubMed: 9736627]
24. Valerie K, Povirk LF. Regulation and mechanisms of mammalian double-strand break repair. Oncogene 2003;22:5792–812. [PubMed: 12947387]
25. An J, Yang DY, Xu QZ, Zhang SM, Huo YY, Shang ZF, et al. DNA-dependent protein kinase catalytic subunit modulates the stability of c-Myc oncoprotein. Mol Cancer 2008;7:32. [PubMed: 18426604]
26. Tang X, Yuan F, Guo K. Repair of radiation damage of U2OS osteosarcoma cells is related to DNA-dependent protein kinase catalytic subunit (DNAPKcs) activity. Mol Cell Biochem 2014;390:51–9. [PubMed: 24390088]
27. Gustafsson AS, Abramenkovs A, Stenerlow B. Suppression of DNA-dependent protein kinase sensitize cells to radiation without affecting DSB repair. Mutat Res 2014;769:1–10. [PubMed: 25771720]
28. Nagasawa H, Little JB, Lin YF, So S, Kurimasa A, Peng Y, et al. Differential role of DNA-PKcs phosphorylations and kinase activity in radiosensitivity and chromosomal instability. Radiat Res 2011; 175:83–9. [PubMed: 21175350]

29. Willmore E, Elliott SL, Mainou-Fowler T, Summerfield GP, Jackson GH, O'Neill F, et al. DNA-dependent protein kinase is a therapeutic target and an indicator of poor prognosis in B-cell chronic lymphocytic leukemia. Clin Cancer Res 2008;14:3984–92. [PubMed: 18559621]

30. Abdel-Fatah TM, Arora A, Moseley P, Coveney C, Perry C, Johnson K, et al. ATM, ATR and DNA-PKcs expressions correlate to adverse clinical outcomes in epithelial ovarian cancers. BBA Clin 2014; 2:10–7. [PubMed: 26674120]

31. Cornell L, Munck JM, Alsinet C, Villanueva A, Ogle L, Willoughby CE, et al. DNA-PK-A candidate driver of hepatocarcinogenesis and tissue biomarker that predicts response to treatment and survival. Clin Cancer Res 2015;21:925–33. [PubMed: 25480831]

32. Dolman ME, van der Ploeg I, Koster J, Bate-Eya LT, Versteeg R, Caron HN, et al. DNA-dependent protein kinase as molecular target for radiosensitization of neuroblastoma cells. PLoS One 2015;10: e0145744. [PubMed: 26716839]

33. Bouchaert P, Guerif S, Debiais C, Irani J, Fromont G. DNA-PKcs expression predicts response to radiotherapy in prostate cancer. Int J Radiat Oncol Biol Phys 2012;84:1179–85. [PubMed: 22494583]

34. Goodwin JF, Kothari V, Drake JM, Zhao S, Dylgjeri E, Dean JL, et al. DNA-PKcs-mediated transcriptional regulation drives prostate cancer progression and metastasis. Cancer Cell 2015;28: 97–113. [PubMed: 26175416]

35. Kase M, Vardja M, Lipping A, Asser T, Jaal J. Impact of PARP-1 and DNAPK expression on survival in patients with glioblastoma multiforme. Radiother Oncol 2011;101:127–31. [PubMed: 21775006]

36. Tichy A, Novotna E, Durisova K, Salovska B, Sedlarikova R, Pejchal J, et al. Radio-sensitization of human leukaemic molt-4 cells by DNA-dependent protein kinase inhibitor, NU7026. Acta Medica (Hradec Kralove) 2012;55:66–73. [PubMed: 23101268]

37. Zhao Y, Thomas HD, Batey MA, Cowell IG, Richardson CJ, Griffin RJ, et al. Preclinical evaluation of a potent novel DNA-dependent protein kinase inhibitor NU7441. Cancer Res 2006;66:5354–62. [PubMed: 16707462]

38. Ciszewski WM, Tavecchio M, Dastych J, Curtin NJ. DNA-PK inhibition by NU7441 sensitizes breast cancer cells to ionizing radiation and doxorubicin. Breast Cancer Res Treat 2014;143:47–55. [PubMed: 24292814]

39. Quiros S, Roos WP, Kaina B. Rad51 and BRCA2–New molecular targets for sensitizing glioma cells to alkylating anticancer drugs. PLoS One 2011;6: e27183. [PubMed: 22073281]

40. Shaheen FS, Znojek P, Fisher A, Webster M, Plummer R, Gaughan L, et al. Targeting the DNA double strand break repair machinery in prostate cancer. PLoS One 2011;6:e20311. [PubMed: 21629734]

41. Dong J, Zhang T, Ren Y, Wang Z, Ling CC, He F, et al. Inhibiting DNA-PKcs in a non-homologous end-joining pathway in response to DNA double-strand breaks. Oncotarget 2017;8:22662–73. [PubMed: 28186989]

42. Hayat M Brain Metastases from Primary Tumors, vol. 2: Epidemiology, Biology, and Therapy. Boston, MA: Elsevier; 2015.

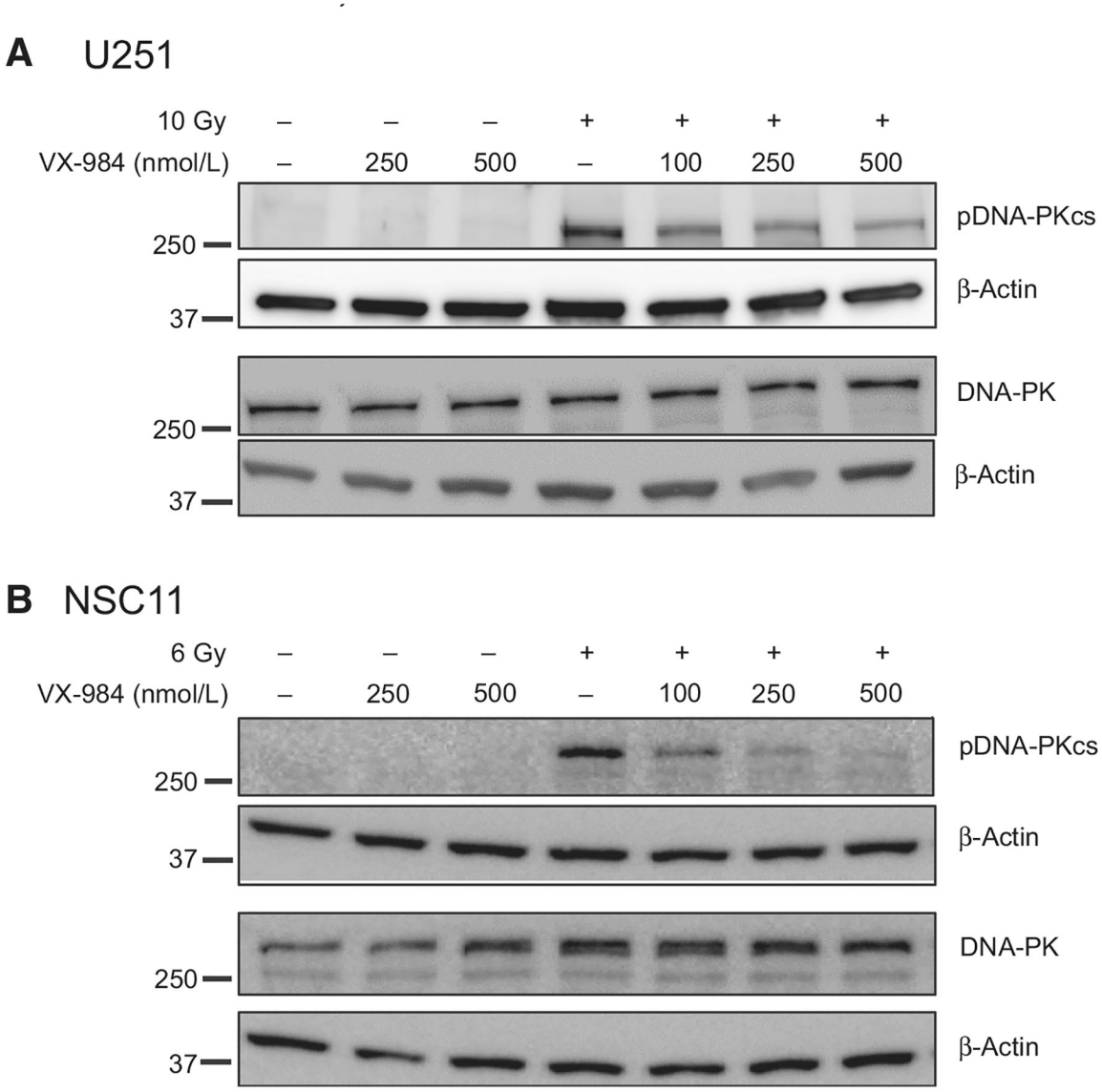

Figure 1.

Effects of VX-984 on DNA-PKcs phosphorylation *in vitro*. **A**, U251 or **B**, NSC11 cells were treated with the specified dose of VX-984 1 hour before irradiation (10 Gy for U251; 6 Gy for NSC11), collected 1 hour after irradiation, and subjected to immunoblot analysis. Blots are representative of two independent experiments.

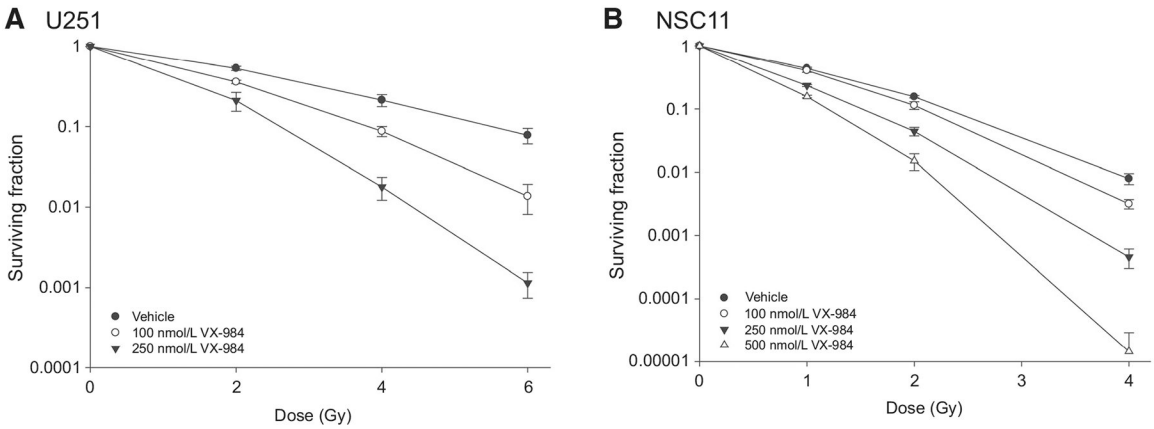

Figure 2.

Effects of VX-984 on radiosensitivity. **A**, U251 or **B**, NSC11 cells were plated as single cells at clonogenic density and allowed to attach overnight. VX-984 was added to culture at the indicated concentration 1 hour before irradiation; 24 hours after irradiation, media were removed and fresh drug-free media were added. Colony-forming efficiency was determined 10 to 12 days later for U251 and 16 to 18 days later for NSC11. Survival curves were generated after normalizing for cell killing induced by VX-984 alone. Values shown represent the means ± SEM for 3 independent experiments.

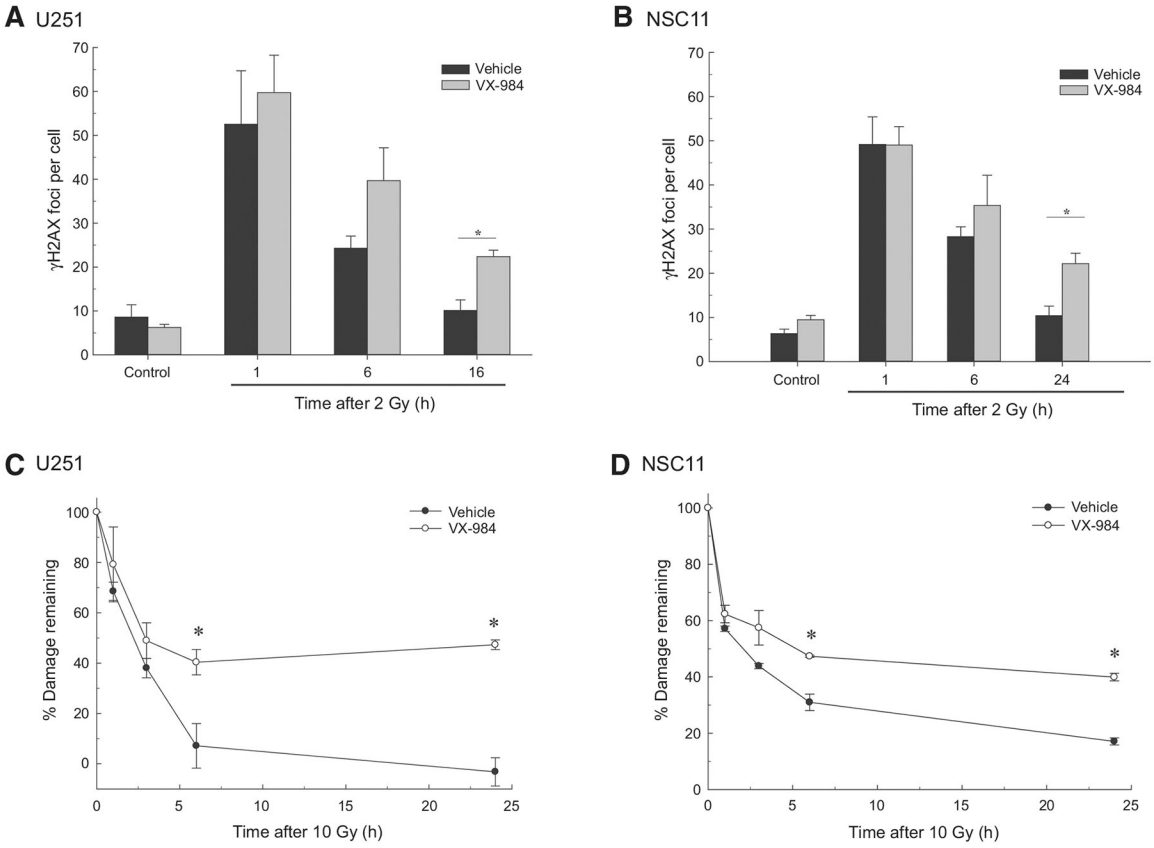

Figure 3.

Influence of VX-984 on DNA DSB repair. **A** to **B**, Radiation-induced gH2AX foci formation and dispersal. U251 (**A**) or NSC11 (**B**) cells were exposed to VX-984 (250 nmol/L for U251; 500 nmol/L for NSC11) 1 hour before irradiation (2 Gy). Cells were collected at the indicated time points for immunofluorescence analysis. gH2AX foci were counted in at least 30 nuclei per condition. **C** to **D**, Neutral comet assay. U251 (C) or NSC11 (D) cells were exposed to VX-984 (250 nmol/L for U251; 500 nmol/L for NSC11) 1 hour before irradiation (10 Gy). Cells were analyzed at times out to 24 hours. Data are expressed as percent damage remaining in which the tail moment immediately after irradiation corresponds to 100% damage. Values shown represent the means ± SEM for 3 independent experiments. *, $P < 0.05$ according to Student t test (VX-984 vs. vehicle).

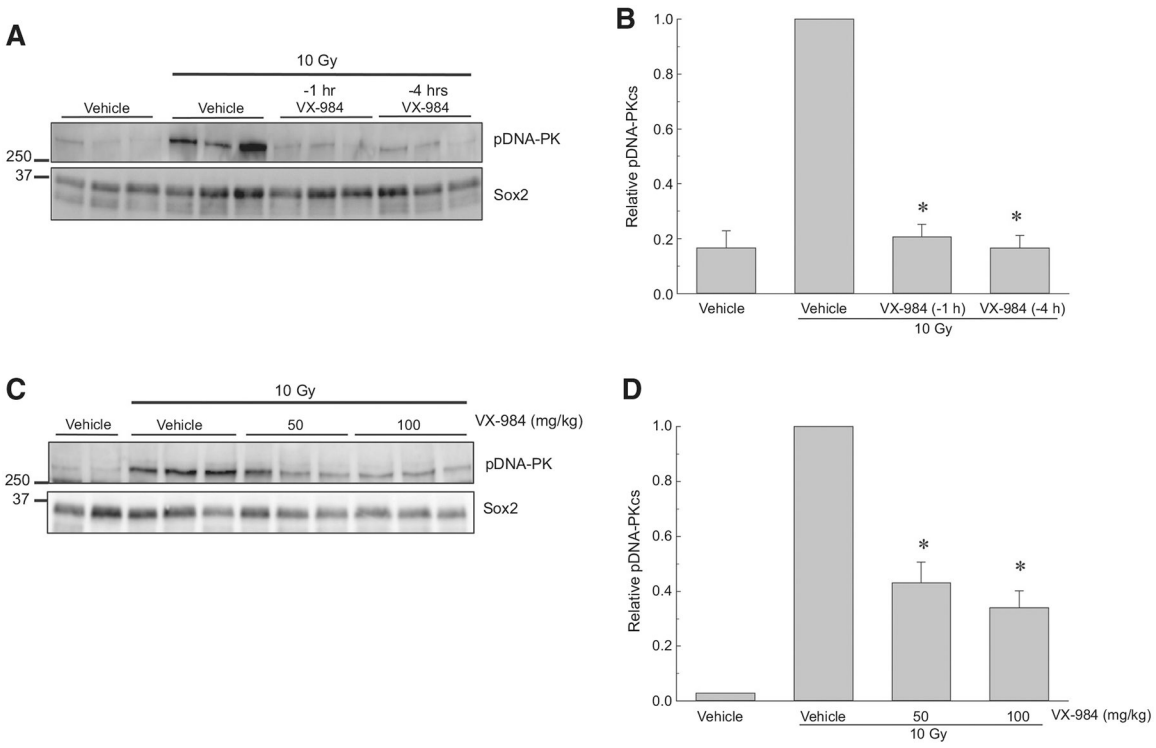

Figure 4.

Effects of VX-984 on DNA-PKcs phosphorylation in orthotopic xenografts initiated from U251 cells. At 18 days after orthotopic implant, mice were randomized according to BLI and treatment initiated 2 days later as described. **A**, Western blot and (**B**) densitometry analysis of pDNA-PKcs levels in tumors collected from mice treated with VX-984 (100 mg/kg) or 5% methylcellulose (vehicle) by oral gavage at 1 or 4 hours before irradiation (10 Gy). **C**, Western blot and (**D**) densitometry analysis of pDNA-PK levels of mice treated with VX-984 (50 mg/kg or 100 mg/kg) or vehicle by oral gavage 4 hours before irradiation (10 Gy). Tumors were collected 1 hour after irradiation for immunoblot analysis. Human-specific Sox2 was used as a loading control, and relative pDNA-PKcs levels were determined by setting the radiation only samples at 1.0. Values shown represent the means ± SEM for 3 mice, *, $P < 0.05$ according to one-tailed Student *t* test (10 Gy þVX-984 vs. 10 Gy).

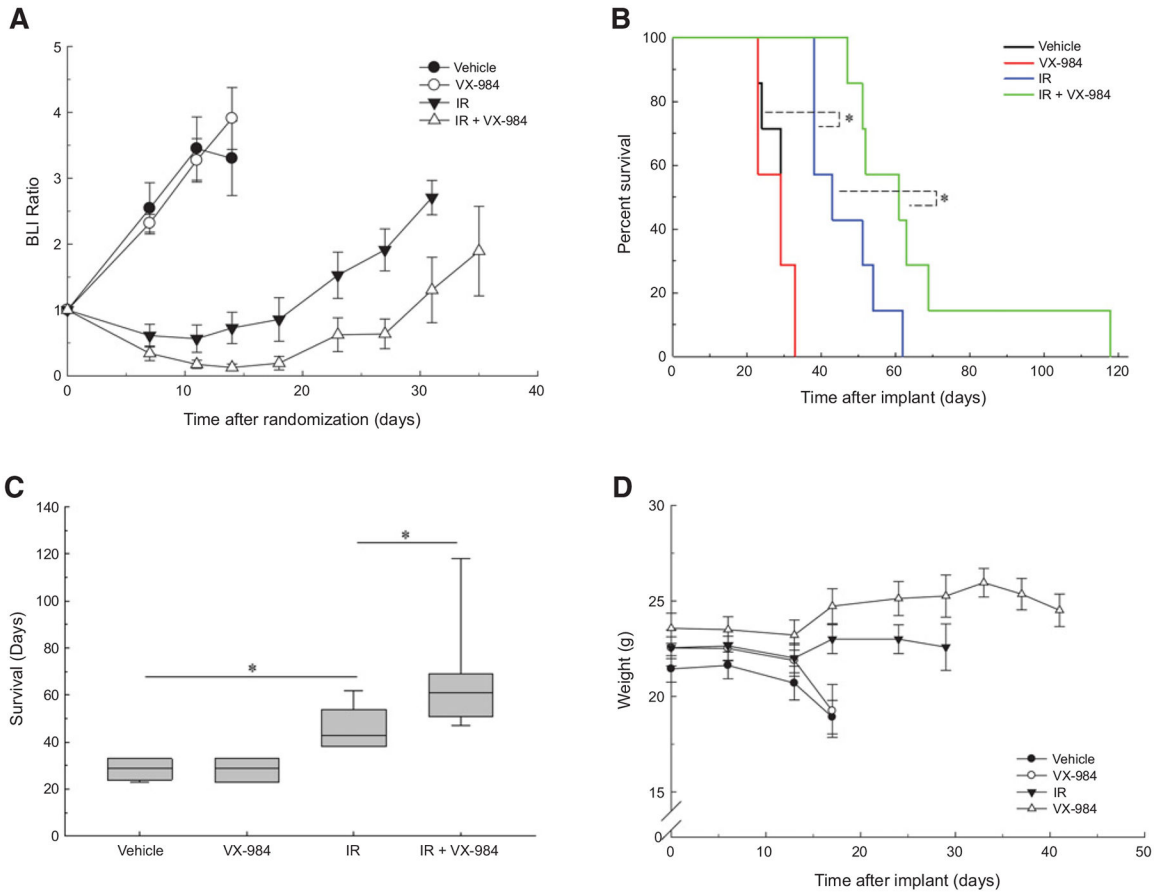

Figure 5.

Influence of VX-984 on the radioresponse of U251 orthotopic xenografts. At 6 days after intracranial implantation initiated from U251 cells, mice were randomized according to BLI and treatment initiated the following day (7 mice/group). Mice were treated with VX-984 (50 mg/kg) or vehicle by oral gavage 30 minutes before and 4 hours after irradiation (3 Gy; IR) for 3 consecutive days. Bioluminescent (BLI) and weight measurements were recorded biweekly until the first onset of morbidity per treatment group. Mice were followed until the onset of morbidity. **A**, BLI measurements of individual groups, values shown represent the means ± SEM. B, Kaplan–Meier survival curves with log-rank analysis for comparison (*, $P = 0.03$). **C**, Boxplot of median survival with Mann–Whitney test (*, $P = 0.04$). **D**, Weight measurements of treatment groups. Values shown represent the means ± SEM.

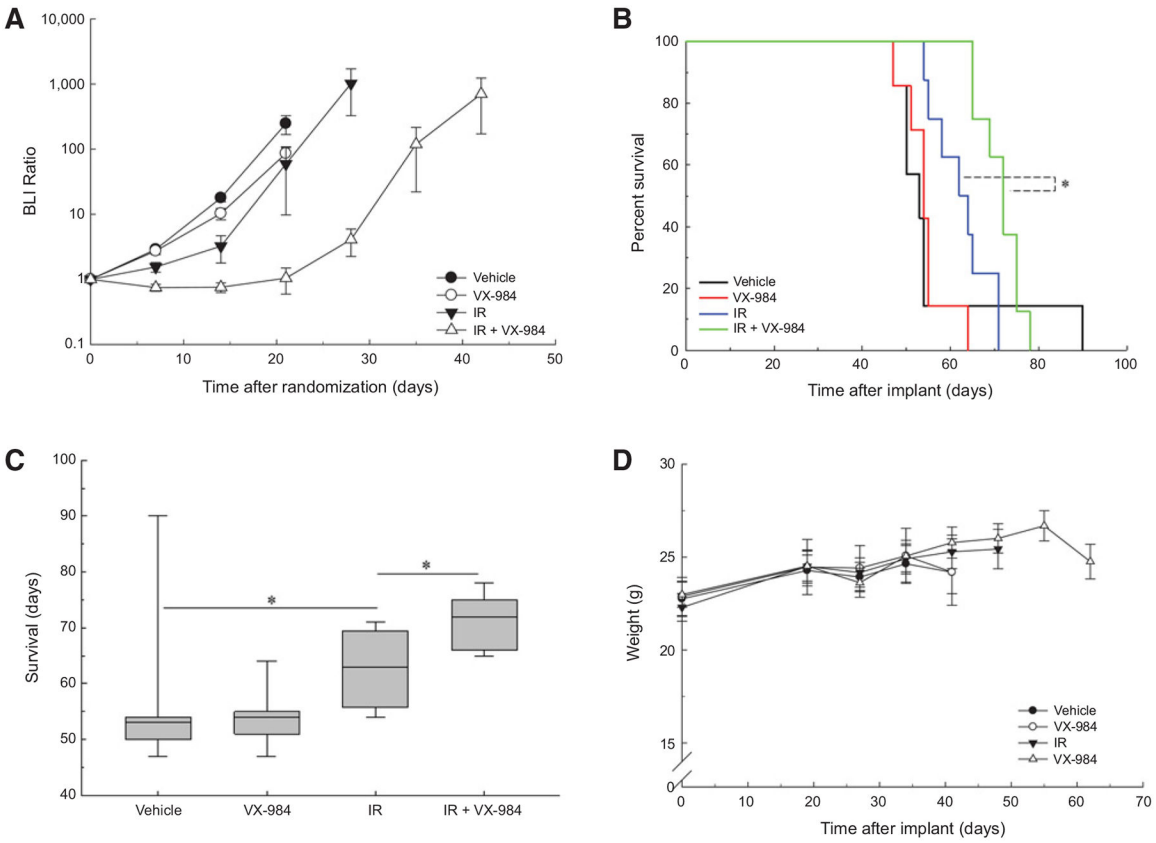

Figure 6.

Influence of VX-984 on the radioresponse of NSC11 orthotopic xenografts. At 20 days after intracranial implantation of $CD133^{+}$ NSC11 cells, mice were randomized according to BLI and treatment initiated the following day (7 mice/group in vehicle and VX-984; 8 mice/group in IR and IR VX-984). Mice were treated with VX-984 (50 mg/kg) or vehicle by oral gavage 30 minutes before and 4 hours after irradiation (3 Gy; IR) for 3 consecutive days. Bioluminescent (BLI) and weight measurements were recorded weekly until the first onset of morbidity per treatment group. Mice were followed until the onset of morbidity. **A**, BLI measurements of individual groups, values shown represent the means SEM. **B**, Kaplan–Meier survival curves with log-rank analysis for comparison ($P = 0.004$). **C**, Boxplot of median survival with Mann–Whitney test ($P = 0.005$). **D**, Weight measurements of treatment groups; values shown represent the means ± SEM.